trapolated to zero scattering angle with more confidence. The translational diffusion coefficient at infinite dilution can be evaluated by using a modified Zimm plot (eq 27 and 28). We observed dilute solution behavior at $C < C_m$, at which concentration $[\Delta R_{vv}/(HC)]$ also shows a minimum. The concentration C_m $[\sim M/(N_A d^* L^{*2})]$ differs from C^{**} $[\sim M/(N_A d L^2)]$ for rigid rods. The solution behavior for semiflexible chains is correlated to the macromolecular size and changes sharply with increasing concentration (Figure 9). Thus, we consider it more reasonable to regard C_m as the threshold concentration from the semidilute to the concentrated solution regime. Furthermore, for wormlike chains, the concentration range between semidilute and concentrated solution regimes is more compressed.

Acknowledgment. We gratefully acknowledge the National Science Foundation, Polymers Program (Grant DMR 8314193) and the Petroleum Research Fund, administered by the American Chemical Society, for support of this research.

Registry No. PPTA (SRU), 24938-64-5; PPTA (copolymer), 25035-37-4; K_2SO_4, 7778-80-5.

References and Notes

(1) Chu, B.; Ying, Q.; Wu, C.; Ford, J. R.; Dhadwal, H.; Qian, R.; Bao, J.; Zhang, J.; Xu, C. *Polym. Commun.* **1984**, *25*, 211.
(2) Ying, Q.; Chu, B.; Qian, R.; Bao, J.; Zhang, J.; Xu, C. *Polymer* **1985**, *26*, 1401.
(3) Chu, B.; Ying, Q.; Wu, C.; Ford, J. R.; Dhadwal, H. S. *Polymer* **1985**, *26*, 1408.
(4) Chu, B.; Wu, C.; Ford, J. R. *J. Colloid Interface Sci.* **1985**, *105*, 473.
(5) Wong, C. P.; Ohnuma, H.; Berry, G. C. *J. Polym. Sci., Polym. Symp.* **1978**, *No. 65*, 173.
(6) Burchard, W.; Eisele, M. *Pure Appl. Chem.* **1984**, *56*, 1379.
(7) Wilcoxon, J.; Schurr, J. M. *Biopolymers* **1983**, *22*, 849.
(8) Broersma, S. J. *J. Chem. Phys.* **1960**, *32*, 1626, 1632.
(9) Stockmayer, W. H.; Schmidt, M. *Pure Appl. Chem.* **1982**, *54*, 407.
(10) Doi, M.; Edwards, S. F. *J. Chem. Soc., Faraday Trans. 2* **1978**, *74*, 560.
(11) Ying, Q.; Chu, B. *Makromol. Chem., Rapid Commun.* **1984**, *5*, 785.
(12) The details will be described separately by: Ying, Q.; Chu, B., to be published.

Application of Raman and Laser Light Scattering to the Melt Polymerization of Hexachlorocyclotriphosphazene. 1

Day-chyuan Lee,† James R. Ford, George Fytas,‡ and Benjamin Chu*

Department of Chemistry, State University of New York at Stony Brook, Long Island, New York 11794-3400

Gary L. Hagnauer

Polymer Research Division, Army Materials Technology Laboratory, Watertown, Massachusetts 02172-0001. *Received November 4, 1985*

ABSTRACT: The application of a novel laser light scattering apparatus is described for on-line monitoring of the high-temperature, melt polymerization of hexachlorocyclotriphosphazene (HCTP) and the in situ characterization of the poly(dichlorophosphazene) (PDP) product. A combination of Raman spectroscopy, angular measurement of absolute light scattering intensities, and Rayleigh line width (dynamic) light scattering measurements are employed. More conventional techniques are inappropriate due to the polymer's hydrolytic instability, the high temperature required for polymerization, and the nature and apparent complexity of the reaction. Concentrations of the reaction components and characteristics of the polymer, such as weight-average molecular weight (M_w) and z-average radius of gyration (R_g) in the dilute solution regime and the cooperative diffusion coefficient (D_c) and osmotic compressibility $[(\partial\Pi/\partial C)_{T,P}]$ in semidilute solutions, are monitored with polymerization time. Experimental results are found to be in excellent agreement with those obtained indirectly by the batchwise polymerization of the same material.

Introduction

Poly(organophosphazenes) comprise a promising new class of technological polymers usually prepared by the organosubstitution of chlorine atoms on poly(dichlorophosphazene) (I).[1-3] The precursor polymer I, a high molecular weight elastomer (T_g, −63 °C), reacts with moisture and therefore must be modified in order to obtain long-term hydrolytic stability and other useful properties. Depending upon the size and nature of the side group substituents, polymers with a wide range of physical properties may be produced.

The polymer I is prepared by the high-temperature (ca. 250 °C) ring-opening polymerization of hexachlorocyclotriphosphazene (II).[4] Polymerizations may be conducted in solution or in the cyclic trimer melt, and catalysts may

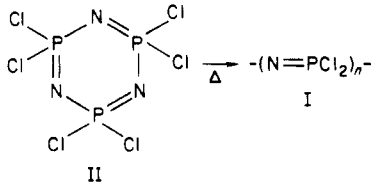

II I

be employed to reduce the reaction temperature and control polymer structure.[4,5] It is essential that II is highly pure and polymerization conditions are carefully controlled. If impurities are present or if the polymerization is allowed to continue too long or at too high a temperature, I may cross-link and thereby be unsuitable for organosubstitution.

The cyclic trimer II is a white crystalline (mp 112–114 °C) solid that sublimes under vacuum and is soluble in most organic solvents. The open-chain polymer I is soluble in a variety of solvents (e.g., benzene, trichlorobenzene, chloroform, and tetrahydrofuran) and typically has a high molecular weight ($M_w = 2 \times 10^6$) and broad molecular weight distribution ($M_w/M_n = 3$–7). Precautions must be

* Author to whom all correspondence should be addressed.
† Present address: Chemical Engineering Department, University of Wisconsin, Madison, Wisconsin 57305.
‡ Present address: Chemistry Department, University of Crete, PO Box 1470, 711 10 Iraklion Crete, Greece.

0024-9297/86/2219-1586$01.50/0

taken in handling and characterizing I due to its sensitivity to moisture. Indeed, dilute solution techniques for characterizing I have been developed only recently.[6-8] Direct monitoring of the polymerization process has been hampered by the high temperature required for polymerization and the apparent complexity of the reaction. Consequently, most polymerization studies have been conducted batchwise.

In this paper a novel on-line laser light scattering technique is described that not only overcomes the difficulties of monitoring the concentrations of I and II but also allows I to be characterized during the course of polymerization. A combination of Raman spectroscopy, absolute light scattering intensity measurements at different scattering angles, and Rayleigh line width (dynamic) light scattering measurements are employed to monitor the polyermization process. From a quality control viewpoint it is important to find a method to characterize the poly(dichlorophosphazene) (PDP) polymer in situ. If the PDP polymer product does not measure up to the expected quality control standard, considerable time and expense could be saved by avoiding the substitution process. Thus, one of our aims is to demonstrate that development of an on-line technique for characterizing the PDP product during the course of the polymerization reaction is within reach.

This paper includes a brief review of the theory of polymer solutions and light scattering in order to provide the equations used in our analysis. The instrumentation for light scattering measurements and experimental procedure for hexachlorocyclotriphosphazene (HCTP) preparation are described. Finally, we report the results of our studies on the thermal polymerization of HCTP.

Theoretical Background

Scaling Relations. The root-mean-square radius of gyration (R_g) can be related to the weight-average molecular weight M_w by a semiempirical scaling relation[9]

$$R_g = k_R M_w^{\alpha_R} \tag{1}$$

where k_R and α_R are constants. α_R has a value of 0.5 at the Θ condition and 0.6 in a good solvent. Thus, α_R also serves as an index of solvent quality.

In the dilute regime individual polymer coils are well separated. At higher concentrations the polymer coils begin to overlap. The threshold concentration at which this happens would be expected to occur when the total volume of the chains just fills the available volume, i.e.

$$C^* \sim M_w/N_A R_g^3 \tag{2}$$

where N_A is Avogadro's number. The overlap concentration C^* scales as $M^{1-3\alpha_R}$, where $1 - 3\alpha_R = -0.5$ in a Θ solvent and -0.8 in a good solvent.

In the semidilute regime ($C > C^*$), the self-excluded volume of a polymer chain is diminished and the polymer chain should behave as an ideal random chain.

In the dilute regime, the osmotic pressure $\Pi^D \sim C/M$, with the superscript D denoting the dilute regime. The value of Π^{SD} in the semidilute (SD) regime is determined by properties due to local segmental concentrations. It does not matter whether the local segmental concentration comes from many chains or from a single chain. Thus the value of Π^{SD} in the semidilute regime must be independent of the molecular weight for high molecular weight polymers, leading to

$$\Pi^{SD} \sim C^m \tag{3}$$

where $m = 1 + 1/(3\alpha_R - 1)$. For a Θ solvent $m = 3$, while for a good solvent $m = {}^9/_4$.

The scaling concept allows us to predict most of the polymer behavior in the semidilute regime empirically.

Intensity of Scattered Light.[10,11] The measurable parameter from light scattering, the Rayleigh ratio, is related to the osmotic pressure through

$$\lim_{K\to 0} HC/R_{vu} = (1/RT)(\partial\Pi/\partial C)_{P,T} \quad \text{(all concentrations)} \tag{4}$$

$$\lim_{K\to 0} HC/R_{vu} = 1/M_w + 2A_2C \quad \text{(dilute regime)} \tag{5}$$

where H (in units of mol cm^2 g^{-2}) is equal to $4\pi^2 n^2 (dn/dC)^2/(N_A\lambda_0^4)$ with n, C (g/cm^3), N_A, λ_0, and dn/dC being respectively the refractive index, the concentration, Avogadro's number, the wavelength of light in vacuo, and the refractive index increment, R_{vu} (cm^{-1}) is the excess Rayleigh ratio due to concentration fluctuations of the polymer solution using vertically polarized incident and unpolarized scattered light, A_2 (mol cm^3 g^{-2}) is the second virial coefficient, and $(\partial\Pi/\partial C)_{T,P}$ is the osmotic compressibility. K [$=(4\pi/\lambda)\sin(\theta/2)$] is the magnitude of the momentum transfer vector, with λ [$=\lambda_0/n$] and θ being the wavelength of light in the scattering medium and the scattering angle, respectively.

By taking interference effects into consideration the Rayleigh ratio (R_{vu}) at finite concentrations in dilute solution has the approximate form

$$HC/R_{vu} = (1/M_w)(1 + K^2R_g^2/3) + 2A_2C \tag{6}$$

In the limit $C \to 0$, eq 6 is reduced to

$$\lim_{C\to 0} HC/R_{vu} = (1/M_w)(1 + K^2R_g^2/3) \tag{7}$$

In the limit $\theta \to 0$, eq 6 is reduced to eq 5. If both C and θ approach 0, eq 6 is reduced to

$$\lim_{\substack{C\to 0\\ \theta\to 0}} HC/R_{vu} = 1/M_w \tag{8}$$

Raman Spectroscopy. In a chemical reaction some bonds are broken and others are being formed, while most remain relatively unchanged. Therefore, Raman peaks that are characteristic of the respective chemicals of interest can be used to monitor the concentrations of those chemicals,[12-16] while the peaks that show no change during the polymerization process can be used to monitor the laser incident intensity and act as some form of an internal built-in reference standard useful for normalization purposes.

Spectrum of Scattered Light.[17] The intensity–intensity time correlation function $G^{(2)}(\tau)$ and the first-order normalized electric field correlation function $g^{(1)}(\tau)$ are closely related through the Siegert relation. For a detector of finite effective photocathode

$$G^{(2)}(\tau) = N_s\langle n\rangle^2(1 + b|g^{(1)}(\tau)|^2) \tag{9}$$

where τ is the delay time, $\langle n\rangle$ is the average number of counts per sample time, and N_s is the total number of samples. The base line $A = N_s\langle n\rangle^2$, and b is a spatial coherence factor, usually taken as an unknown adjustable parameter in the data-fitting procedure. Equation 9 is valid for an extensive class of signals having a Gaussian field probability distribution.

The first-order time correlation function for a monodisperse sample of noninteracting macromolecules in solution has the form

$$g^{(1)}_{UN}(K,\tau) \sim I(K)\exp(-\Gamma(K)\tau) \tag{10}$$

where Γ [$=DK^2$ in the absence of internal motions, with D being the translational diffusion coefficient] is the characteristic line width and the subscript UN denotes

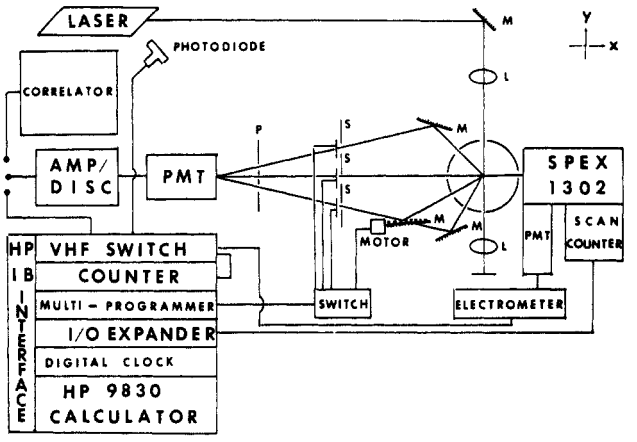

Figure 1. Schematic diagram of the light scattering spectrometer capable of simultaneous measurements of angular distribution of absolute scattered intensity/Rayleigh line width and Raman scattering at high temperatures (up to 350 °C). Additional optical components that are not shown in this schematic diagram: (1) two mirrors that change the beam height suitable for Raman intensity measurements; (2) a number of pinholes to limit stray light. Abbreviations: AMP, amplifier; DISC, discriminator; PMT, photomultiplier; HPIB is the trade name for the Hewlett-Packard IEEE interface. We used a Spectra Physics Model 165 argon ion laser operating at λ_0 = 488 nm and 200 mW.

unnormalized correlation function. For polydisperse polymers

$$\bar{\Gamma} = \int \Gamma G(\Gamma)\, d\Gamma \qquad (11)$$

where $G(\Gamma)$ is a normalized characteristic line width distribution. In semidilute solution, we measured a cooperative diffusion coefficient D_c [$=\bar{\Gamma}/K^2$], which is relatively independent of molecular weight.

Experimental Methods

Light Scattering Spectrometer. The light scattering spectrometer used for this study measures the angular distribution of absolute scattered intensity, the Rayleigh line width, and the Raman intensity. Figure 1 shows a schematic diagram of the automated Raman/light scattering spectrometer.

The cell holder, as shown in Figures 2 and 3, has three parts: an outer cell holder, an intermediate cell holder, and an inner cell holder. The E-shaped outer cell holder was mounted on a series of positioning alignment devices. From top to bottom they are a small homemade rotary stage (F in Figure 2), providing rotational adjustment along the cylindrical z-axis, two Lansing translational stages (G), providing x–y adjustments, and a mini optical table (H, 6 × 6 in.), providing x–y tilt adjustments. The mini optical table was mounted on a homemade aluminum platform fixed to the Modern Optics isolation table and supports all the detection optics needed for intensity/correlation measurements.

The main body of the intermediate cell holder, which was used for viewing the scattering volume, was made from a piece of precision-bore Pyrex glass tubing of 55-mm o.d. A flat window was attached to this section, providing a perpendicular entrance surface for the incident laser beam. To avoid radiative heat loss the intermediate cell holder was evacuated. A stainless steel rod in the platform (M in Figure 3) provided thermal isolation of the inner cell holder.

The inner cell holder rests on the platform in such a way that it could be removed and replaced reproducibly without affecting the alignment. A precision hole bored into this cell holder (J in Figure 3) accommodates a 22-mm-o.d. × 66-mm-long cylindrical scattering cell. Heating wires (G in Figure 3) purchased from ACE Glass were coiled around the inner cell holder (J), and temperature sensors were placed inside slots (I) of the inner cell holder. An Artronix Model 5301 temperature controller was used to control the temperature to ±0.05 °C at 250 °C.

In detecting the scattered light, as shown in Figure 1, the spectrometer used three mirrors (M) to direct light at scattering

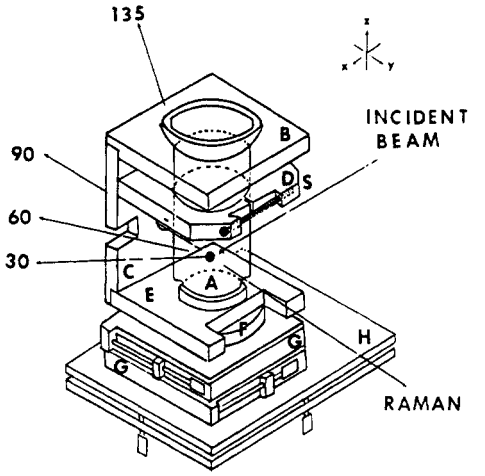

Figure 2. Schematic diagram of the thermostated outer cell holder for the scattering spectrometer: (A) intermediate cell holder; (B) top piece of outer cell holder; (C) side piece of cell holder; (D) middle piece of cell holder, with a slit that can be tightened by a screw S to properly hold the light scattering cell; (E) bottom piece of cell holder; (F) small rotational rotary table (around the z axis); (G) two micrometer stages, allowing adjustments of the cell position in the x–y direction; (H) small optical table, allowing tilt adjustments of the cylindrical cell.

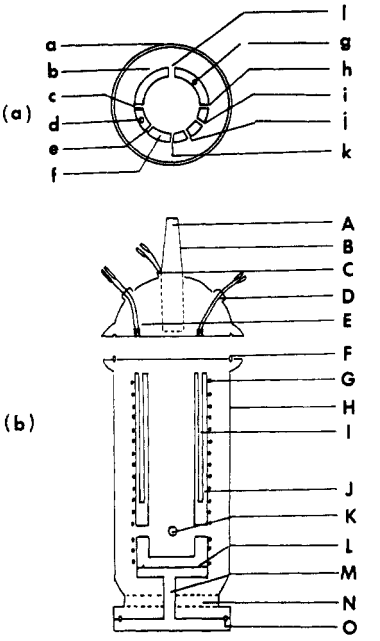

Figure 3. Schematic diagram of the thermostated inner cell holder for the scattering spectrometer. Part a represents the cross section parallel to the surface of the optical table at the height of the incident beam. Part b is the cross section of the cell perpendicular to the optical table and passes through the scattering volume. Top view: (a) outer glass; (b) vacuum; (c) light entrance; (d) slot for thermistor; (e) opening at 135° scattering angle; (f) inner cell holder; (g) slot for thermistor; (h) exit slit; (i) opening at 30° scattering angle; (j) opening at 60° scattering angle; (k) opening at 90° scattering angle; (l) opening for Raman. Side view: (A) glass neck for connection to vacuum tube; (B) top portion of the glass holder; (C) connection for heating wire; (D) connection for temperature control probe; (E) connection for thermometer; (F) o-ring; (G) heating wire; (H) bottom portion of the glass vacuum jacket; (I) slot for thermistor (as in d and g of part a); (J) inner cell holder; (K) opening for Raman; (L) positioning pin; (M) inner cell holder platform; (N) Kovar glass; (O) o-ring.

angles 30°, 60°, and 135° to the photomultiplier tube (PMT). These three mirrors were set on aluminum posts directly mounted on the Modern Optics isolation table. The mirror for the 60° scattering angle could be moved (forward and backward) by a

motor in order to share the same detection optics with the 30° scattering beam. Three slits, three electronic shutters, and three pinholes were mounted on the platform, as shown in Figure 1, with a Centronic photomultiplier tube (P4249B) at the far end.

Data Collection. The electronics for intensity and line width measurements, as shown in Figure 1, included an Ortec Model 9301 preamplifier and an Ortec Model 9302 amplifier discriminator for photon counting. The signal was sent via a Hewlett-Packard (HP) 59307A VHF switch (in order to share the HP 5328A universal counter with other devices) to a HP 5328A universal counter. The output from the photodiode was amplified and the voltage was sent via the same HP 59307A VHF switch to the same HP 5328A universal counter. An HP 6940B multiprogrammer was used to control the on/off sequence of an Apcor Model 220130 gear motor (to move the mirror for θ at 60°) and the three electric shutters used to choose the desired scattering angle. Raman spectra were obtained by using a Spex 1302 double monochrometer (0.5 m, 1200 grooves/mm), and interfaced through an HP9868A I/O expander to control the scan. The output of the Raman signal was first sent to a Keithley Model 615 digital electrometer, which was connected via the HP 59307A VHF switch. The entire system was automated through an HP 9830 calculator via the HP-IB interface. An HP 59309A HP-IB digital clock was used for timing the experiment. Dynamic measurements were not taken automatically, as some of the parameters needed by the correlator change during the polymerization process. Two correlators were used in this experiment—the single-clipped Malvern K7023 correlator and the Brookhaven Instruments BI-2030 full ($4 \times n$) digital correlator. Samples of benzene and of NBS 705 polystyrene dissolved in benzene were used to check the performance of the instrument.

Sample Preparation. HCTP was obtained from Ethyl Corp. (Ferndale, MI) and was purified by vacuum distillation, recrystallization from heptane, and vacuum sublimation.

Melt polymerization reactions were run in sealed optical glass cells at 250 °C. The molten trimer was filtered through a specially designed, ultrafine (0.8 μm) glass filter apparatus at about 130 °C under nitrogen pressure into the ampules and sealed under vacuum. Typically, the ampules contained 8 g of the trimer.

Physical Constants. We used benzene as a reference for computing the Rayleigh ratio R_{vu} and took $R_{vu} = R_{vv} + R_{vh} = 3.86 \times 10^{-5}$ cm^{-1} [10] for benzene at $\theta = 90°$, $\lambda_0 = 488$ nm, and 23 °C.

HCTP. HCTP is a white crystalline solid (mp, 114 °C). The density of HCTP was estimated by weighing known amounts of HCTP and measuring the volume occupied by liquid HCTP at elevated temperatures. Trichlorobenzene was used as our standard to calibrate the volume of the measuring device at different temperatures. The densities of HCTP were measured at 140, 170, and 200 °C, and least-squares fitted yielding d_m (g/cm^3) = $2.05 - 3.01 \times 10^{-3} t_c$, with t_c expressed in degrees Celsius. The refractive index of HCTP was estimated by shifting our light scattering cell away from the scattering center a small distance and comparing the deviation of the transmitted beam over a very long distance with that of a set of known refractive index liquids. The refractive index of HCTP was measured at three different temperatures (140, 170, and 200 °C) and fitted with linear least squares. The result $n_m = 1.62 - 6.71 \times 10^{-4} t_c$ at wavelength 488 nm was obtained.

PDP. The density of amorphous PDP[19] is 1.98 g/cm^3 at 273 K. This polymer has a glass transition temperature of −63 °C. In order to estimate the temperature dependence of the density, an empirical equation $\alpha_1 T_g = 0.16$ was used,[20,21] where T_g is the glass transition temperature expressed in K and α_1 is the thermal expansion coefficient defined by $(1/V)(\partial V/\partial T)_p$. Thus, d_p (g/cm^3) $= 1.98 \exp(-7.62 \times 10^{-4} t_c)$ was obtained.

The refractive index increment of PDP in TCB solution was measured at three different temperatures. At 30 °C, we used a Brice Phoenix differential refractometer. At 140 and 170 °C, we measured the refractive index using the same principle as with the determination of the refractive index for HCTP and the expression $(dn/dC) = (n_c - n_s)/C$, with subscripts c and s denoting solution and solvent, respectively.

Results and Discussion

Raman spectra were used to determine the concentration of the reactant (C_m) and the product (C_p). Since the amount of product formed was a function of time, the kinetics of the polymerization processes can be studied in terms of the fractional conversion of the polymer (eq 14). In dilute solutions, we can make full use of light scattering intensity (R_{vu}) and line width ($G^{(2)}(\tau)$) data to obtain many of the pertinent molecular parameters such as M_w and R_g of the polymer formed during the polymerization process.

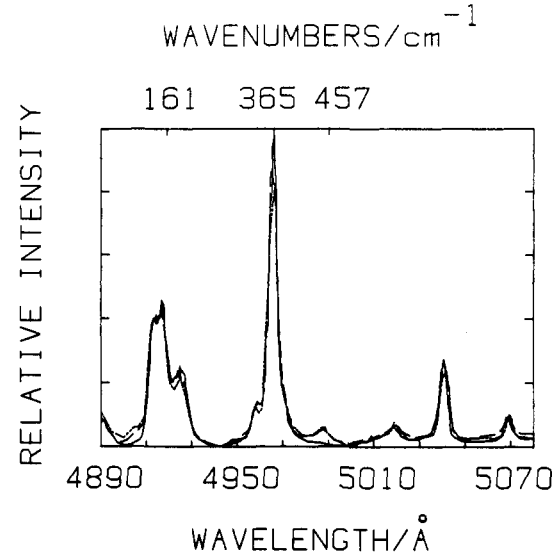

Figure 4. Several Raman spectra obtained during the course of thermal polymerization of hexachlorocyclotriphosphazene at 250 °C showing a decrease in the PCl_2 symmetric stretching peak at 365 cm^{-1}, the constant intensity in the PCl_2 rocking at 161 cm^{-1}, and a polymer peak at 457 cm^{-1} for sample T5 at 1.4 h (solid line), at 42 h (dashed line), and at 61 h (dash-dot line).

Physical Constants. Before we discuss the spectral measurements, several remarks should be made on the physical constants of the PDP polymer. The density of PDP at 250 °C was estimated by using a semiempirical equation (as described in the previous section) to correct for the density change of PDP from 0 to 250 °C. This estimation will appear in calculating the polymer concentration and the refractive index increment. In calculating the polymer concentration, the polymer density is of negligible importance.

Fractional Conversion of Monomer. Initially the Raman spectra of the monomer HCTP and of the polymer PDP were measured.[22-24] The 161-cm^{-1} peak due to the Cl–P–Cl bond bending was chosen as our internal standard and the Cl–P–Cl symmetric stretching at 365-cm^{-1} as a probe for the monomer concentration. Figure 4 shows several Raman spectra obtained during the thermal polymerization of HCTP at 250 °C. The decreasing monomer peak at 365 cm^{-1} with increasing time shows that monomers are being used up during the polymerization process, while the relatively constant peak of the Cl–P–Cl bending at 161 cm^{-1} confirms that our entire light scattering system has remained stable over an extended period of time, i.e., over a period of 15 days. Laser intensity stability is not an important issue here because we can always use the internal reference, Cl–P–Cl bending, to normalize the intensities of other peaks of interest. The polymer peak at 457 cm^{-1} reveals the formation of PDP. However, in the initial stages, the appearance of a polymer peak has a relatively low signal-to-noise ratio. Thus, a direct determination of the polymer concentration is very difficult to obtain from the appearance of a Raman peak when the polymer concentration is low. It should be recognized that the polymer peak could yield useful information as the polymerization process progresses toward its complete conversion. However, we have not used the polymer peak in our present study.

Table I
Fitting Parameters in Evaluating the Time Dependence of Fractional Conversion of Monomer during the Initial Thermal Polymerization of HCTP[a]

sample	$a_1 \times 10^3$, h^{-1}	sample	$a_1 \times 10^3$, h^{-1}
T1	3.23	T5	2.63
T2	3.80	T6	3.40
T3	2.35	T7	2.01
T4	6.84		

[a] $f_p = 1 - \exp(-a_1 t)$.

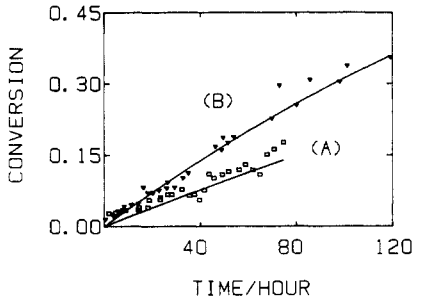

Figure 5. Fractional conversion of polymer vs. time obtained from the height change of PCl_2 peak for sample T6 (inverted triangles, experimental data, solid line A fitted curve) and sample T7 (hollow squares, experimental data, solid line B fitted curve) at 250 °C. The solid lines A and B for samples T7 and T6 were fitted according to eq 14 with a_1 values listed in Table I.

In the Raman spectra, we have observed that the shape of the Raman peaks and the half-width of the monomer characteristic peak at 365 cm^{-1} as well as that of the PCl_2 bending at 161 cm^{-1} remain relatively unchanged. Although the fractional conversion of the monomer can best be determined by using the ratio of the integrated peak area of the PCl_2 stretching intensity at 365 cm^{-1} to that of the PCl_2 bending reference peak at 161 cm^{-1}, we have used the PCl_2 symmetric stretching peak height h_m and normalized it by the PCl_2 bending peak height h_r in order to obtain the fractional conversion of the monomer f_m ($\equiv C_m/(C_m + C_p)$) and the fractional conversion of the polymer f_p ($=1 - f_m = C_p/(C_m + C_p)$) with

$$f_m(t) = h_m(t)h_r^0/h_r(t)h_m^0 \tag{12}$$

where the superscript zero represents the peak height values at time $t = 0$. In order to get the correct height of the reference peak, we have assumed that the Raman peak has a Lorentzian shape and subtracted the contribution of the overlapping neighboring peak from that of the reference peak. The concentration of polymer formed in thermal polymerization, C_p (g/cm^3), has the form

$$C_p = \frac{f_p d_m d_p}{f_p d_m + f_m d_p} \tag{13}$$

where d_m and d_p are densities of HCTP and of PDP, in g/cm^3, respectively. In eq 13, we have assumed no interaction between HCTP and PDP; i.e., the volume of mixing is zero. At high concentrations of PDP this assumption may not be justified. A typical plot of initial fractional conversion of polymer as a function of time can be represented by

$$f_p = 1 - \exp(-a_1 t) \tag{14}$$

with the numerical values for a_1 listed in Table I. Figure 5 shows plots of fractional conversion of polymer vs. time for samples T6 and T7. It should be noted that the reaction rate is affected by only a trace amount of moisture or impurity in HCTP. This is one of the reasons why the proposed scheme will be useful for monitoring the polymerization process of HCTP. The monomer conversion results in thermal polymerization were also checked by comparing the Raman determination with the GPC[8] determination of the final product. It is noted that the first-order rate constants a_1 summarized in Table II are quite similar to the value 3.0×10^{-3} h^{-1} calculated from data obtained in the batchwise polymerization study.[8] We used the Raman technique from an empirical approach, i.e., as an indicator of polymer concentration with calibration by the GPC method. It would require a separate experiment to establish the limitation on the Raman technique for low molecular weight polymers. However, as the Raman technique measures structural changes, it is anticipated that this approach is applicable over a very wide molecular weight range, certainly for polymers of interest in this article.

Table II
Comparison of Fractional Conversion of Monomer during the Thermal Polymerization of Hexachlorocyclotriphosphazene Measured by Raman (in situ) and HPLC (upon Termination of the Polymerization Reaction)

sample	Raman, %	HPLC, %
T1	28.2	27.3
T2	46.3	49.1
T3	47.4	51.3
T4	79.9	86.5
T5	14.9	15.1

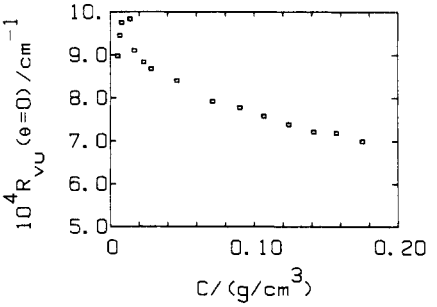

Figure 6. Rayleigh ratio $R_{vu}(\theta=0)$ vs. concentration (g/cm^3) for sample T7. Note R_{vu} here is not the excess Rayleigh ratio where the scattered intensity due to solvent has been subtracted.

Light Scattering Results. The concentration dependence of the Rayleigh ratio $R_{vu}(\theta=0)$ for PDP in HCTP solution at 250 °C is shown in Figure 6. In order to extract the correct Rayleigh ratio for pure HCTP at 250 °C, we measured the Rayleigh ratio R_{vv} and R_{vh} for 1,2,4-trichlorobenzene (TCB) and 50 wt % of HCTP in TCB at 30, 80, 120, and 150 °C, respectively. The depolarization ratio[10] ρ_v and ρ_u can be defined as $\rho_v = R_{vh}/R_{vv}$ and $\rho_u = 2\rho_v/(1 + \rho_v)$, where R_{vh} is the Rayleigh ratio of vertically polarized incident and horizontally polarized scattered light and R_{vv} is the Rayleigh ratio of vertically polarized incident and vertically polarized scattered light.

Depolarization ratios of $\rho_v = 0.26$ ($\rho_u = 0.41$) and $\rho_v = 0.23$ ($\rho_u = 0.37$) were obtained for TCB and 50 wt % HCTP in TCB, respectively. The ratios are insensitive to temperature in the range of our measurements. With the measured depolarization ratio, the Rayleigh ratio R_{vu} can be related to R_{vv} through

$$R_{vu} = R_{vv}/(1 - \tfrac{1}{2}\rho_u) \tag{15}$$

Rayleigh ratios at 250 °C, $R_{vu} = 6.8 \times 10^{-5}$ cm^{-1} and $R_{vu} = 1.82 \times 10^{-4}$ cm^{-1}, were determined for TCB and 50 wt % HCTP in TCB by extrapolation of R_{vv} values to 250 °C and eq 15. A Rayleigh ratio of $R_{vu} = 1.42 \times 10^{-4}$ cm^{-1} was measured for 30% HCTP in TCB at 215 °C. With the assumption that the Rayleigh ratios R_{vu} for 30% and 50%

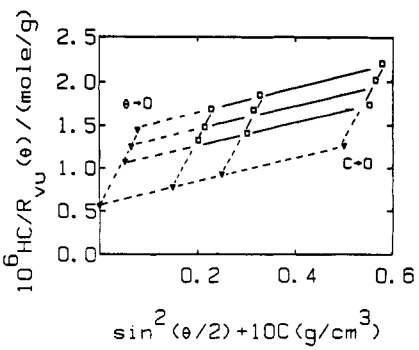

Figure 7. Zimm plot for sample T7, pure HCTP polymerized at 250 °C and measured at 250 °C. From the Zimm plot, we could estimate $M_w \simeq 1.8 \times 10^6$, $A_2 \cong 1.1 \times 10^{-4}$ mol cm^3 g^{-2}, and $R_g \simeq 74$ nm.

HCTP have the same temperature dependence, a R_{vu} value of 1.52×10^{-4} cm^{-1} was estimated for 30% HCTP in TCB at 250 °C. From known values of TCB, 30% HCTP/TCB, and 50% HCTP/TCB, a value of $R_{vu} = 2.8 \times 10^{-4}$ cm^{-1} was estimated for pure HCTP at 250 °C by linear extrapolation. This value can be cross-checked by comparing the isotropic Rayleigh ratio for 30% HCTP/TCB and 50% HCTP/TCB, where[25]

$$R_{iso} = R_{vu}(1 - {}^7/_6\rho_u) \tag{16}$$

and

$$R_{iso} = \frac{\Pi^2 k_B T \beta [\rho(\partial\epsilon/\partial\rho)_T]^2}{2\lambda_0^4} \tag{17}$$

with ϵ and β being the optical dielectric constant and the coefficient of isothermal compressibility, respectively.

The factor $\rho(\partial\epsilon/\partial\rho)_T$ can be estimated by using the Eykmann expression[11]

$$\rho(\partial\epsilon/\partial\rho)_T = \frac{(2n_s^2 + 0.8n_s)(n_s^2 - 1)}{n_s^2 + 0.8n_s + 1} \tag{18}$$

where n_s is the refractive index of the solvent mixture.

β for the solvent mixture can be related to β values of the pure components, β_t and β_m, where the subscripts t and m represent TCB and HCTP, respectively,

$$\beta = \frac{d_m x_t \beta_t + d_t x_m \beta_m}{d_m x_t + x_m d_t} \tag{19}$$

where d and x are the density and the weight fraction, respectively. Therefore, from the Rayleigh ratios of 30% and 50% HCTP in TCB, the Rayleigh ratio for pure HCTP can be estimated as 1.7×10^{-4} cm^{-1} at 250 °C.

Using an average of the estimated R_{vu} values at 250 °C (2.3×10^{-4} cm^{-1}) for pure HCTP from the two approaches, we were able to construct a Zimm plot as shown in Figure 7. We estimated $M_w \simeq 1.8 \times 10^6$, $A_2 \simeq 1.1 \times 10^{-4}$ mol cm^3 g^{-2}, and $R_g = 74 \pm 5$ nm. The uncertainties in R_{vu} for pure HCTP represent uncertainties in the molecular parameters as follows: $1.5 \times 10^6 < M_w < 2.2 \times 10^6$, $6 \times 10^{-5} < A_2$ (mol cm^3 g^{-2}) $< 1.3 \times 10^{-4}$, and $71 < R_g$ (nm) < 79. The M_w and R_g values for PDP are in amazingly good agreement with the values $M_w = 2.1 \times 10^6$ and $R_g = 83$ nm obtained in the batchwise thermal polymerization study.[8]

The universal curve in the good-solvent limit can be described by a continuous curve and has the form

$$\frac{M_w}{RT}\left(\frac{\partial\Pi}{\partial C}\right) = 1 + \frac{1}{8}\left\{9X - 2 + \frac{2\ln(1+X)}{X} \times \exp\left\{\frac{1}{4}\left[\frac{1}{X} + 1 - \frac{1}{X^2}\ln(1+X)\right]\right\}\right\} \tag{20}$$

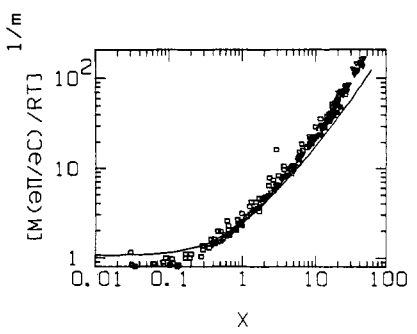

Figure 8. log–log plot of $[M(\partial\Pi/\partial C)/RT]^{1/m}$ vs. X for PST in MEK and PST in toluene (hollow squares), sample PDP/HCTP (filled squares), and PMMA in MMA (inverted hollow triangles). Solid line was calculated according to eq 20. Note: PST/MEK and PST/toluene data were taken from ref 36 and scaled by $m = 1.12$. PMMA/MMA data were taken from ref 35 and scaled by $m = 1.61$. PDP/HCTP data were scaled by $m = 1.16$. The theoretical curve was scaled by $m = 1.10$.

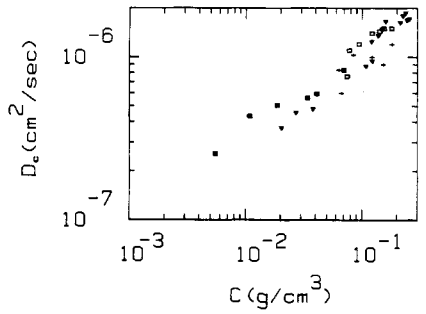

Figure 9. log–log plots of cooperative diffusion coefficient D_c vs. concentration for sample T6 measured at $\theta = 30°$ (inverted filled triangles), sample T6 at $\theta = 60°$ (filled squares), T7 at $\theta = 45°$ (hollow squares), and sample T7 at $\theta = 60°$ (plus signs).

where $X = Q(C/C^*)$ with Q being a constant. Q can be estimated by expanding eq 20 of ref 26 to first order in X

$$X[{}^9/_{16} - {}^1/_8 \ln(M_w/M_n)] \cong A_2 M_w C \tag{21}$$

Figure 8 shows a comparison between the theory, our PDP in HCTP and the literature data on PMMA/MMA,[27] polystyrene (PST)/toluene,[28] and PST/MEK.[28] In order to make a comparison among different solvent qualities, we arbitrarily scaled the y axis to a power of $1/m$, where m is the slope of the curve in the semidilute region from a log–log plot of $M(\partial\Pi/\partial C)/RT$ vs. C/C^*. It should also be noted that from the calculations we should have $Q = 2.6$ and 16 for PDP/HCTP and PMMA/MMA, respectively. However, we used $Q = 1$ and 6 for PDP/HCTP and PMMA/MMA in order to get a better fit. A remarkable agreement between all experimental results and the theory is observed. The agreement also strengthens our experimental results on the PDP/HCTP system because, in order for the agreement to hold, we must have measured correctly both the absolute light scattering intensity and the polymer concentration (by the Raman technique) over a very broad dynamic range.

Figure 9 shows results of the cooperative diffusion coefficient D_c ($=\bar{\Gamma}/K^2$), which has a K^2 dependence and is relatively independent of molecular weight. The results are sufficiently scattered, so no further discussion is warranted.

In conclusion, we have demonstrated that Raman spectroscopy is a useful tool for studying polymerization processes, even for the melt polymerization of HCTP at 250 °C. By combining Raman scattering with light scattering, we have succeeded in characterizing some of the molecular parameters, such as M_w, A_2, and R_g of PDP,

provided that PDP is linear or has a constant degree of branching. As the melt HCTP was difficult to clarify, we have not been able to determine R_{vu} for pure HCTP directly. However, we did succeed in determining R_{vu} for HCTP by two independent methods (to within 50%). Fortunately, at sufficiently high PDP concentration in HCTP, R_{vu} (solution) $\gg R_{vu}$(HCTP). Thus, we were able to estimate the excess Rayleigh ratio in the dilute solution regime. Time correlation function measurements are feasible. However, very precise measurements that could warrant correlation function profile analysis were not made because the melt could not be prepared as dust-free as the monomer in TCB solution. Some cooperative diffusion coefficient results are presented. Future results refer to the solution polymerization of HCTP (Paper 2) for a more detailed and fruitful analysis.

Acknowledgment. We gratefully acknowledge support of this work by the US Army Research Office and the Army Materials Technology Laboratory. G.F. thanks B.C. for his hospitality while working in his laboratory.

Registry No. I (SRU), 26085-02-9; II, 940-71-6; II (homopolymer), 25231-98-5.

References and Notes

(1) Allcock, H. R. *Chem. Eng. News* **1985**, *63*, 22.
(2) Singler, R. E.; Hagnauer, G. L.; Sicka, R. W. *ACS Sym. Ser.* **1984**, *260*, 143.
(3) Singler, R. E.; Hagnauer, G. L.; Sicka, R. W. *ACS Symp. Ser.* **1982**, *193*, 229.
(4) Hagnauer, G. L *J. Macromol. Sci. Chem.* **1981**, *A16* (1), 385.
(5) Sennett, M. S.; Hagnauer, G. L.; Singler, R. E.; Davies, G. *Macromolecules*, in press.
(6) Hagnauer, G. L.; Singler, R. E.; *Org. Coat. Plast. Chem.* **1979**, *44*, 88.
(7) Hagnauer, G. L. *ACS Symp. Ser.*, **1980**, *138*, 239.
(8) Hagnauer, G. L.; Koulouris, T. N. *Chromatogr. Sci.* **1981**, *19*, 99.
(9) de Gennes, P.-G. *Scaling Concepts in Polymer Physics*; Cornell University: Ithaca, NY, 1979; Chapter 1, pp 29-53.
(10) Huglin, M. B., Ed. *Light Scattering from Polymer Solutions*; Academic: New York, 1972.
(11) Kerker, M. *Scattering of Light and Other Electromagnetic Radiation*; Academic: New York, 1969.
(12) Chu, B.; Fytas, G.; Zalczer, G. *Macromolecules* **1981**, *14*, 395.
(13) Sears, W. M.; Hunt, J. L.; Stevens, J. R. *J. Chem. Phys.* **1981**, *75*, 1589.
(14) Sears, W. M.; Hunt, J. L.; Stevens, J. R. *J. Chem. Phys.* **1981**, *75*, 1599.
(15) Gulari, E.; Mckeigue, K.; Ng, K. Y. S. *Macromolecules* **1984**, *17*, 1822.
(16) Loy, B. R.; Chrisman, R. W.; Nyquist, R. A.; Putzig, C. L. *Appl. Spectrosc.* **1979**, *23*, 174.
(17) Chu, G. *Laser Light Scattering*; Academic: New York, 1974. Berne, B. J.; Pecora, R. *Dynamic Light Scattering*; Wiley: New York, 1976.
(18) Chu, B. In *Scattering Techniques Applied to Supramolecular and Nonequilibrium Systems*; Chen, S.-H., Chu, B., Nossal, R., Eds.; Plenum: New York, 1981, pp 231-264.
(19) Allcock, H. R.; Arcus, R. A. *Macromolecules* **1979**, *12*, 1130.
(20) Simha, R.; Boyer, R. F. *J. Chem. Phys.* **1962**, *37*, 1003.
(21) Boyer, R. F.; Spencer, R. S. *J. Appl. Phys.* **1944**, *15*, 398.
(22) Painter, P. C.; Zarian, J.; Coleman, M. M. *Appl. Spectrosc.* **1982**, *36*, 265.
(23) Zarian, J.; Painter, P. C.; Coleman, M. M. *Appl. Spectrosc.* **1982**, *36*, 272.
(24) Coleman, M. M.; Zarian, J.; Painter, P. C. *Appl. Spectrosc.* **1982**, *36*, 277.
(25) Huglin, M. B.; Sokro, M. B. *Polymer* **1980**, *18*, 651.
(26) Ohta, T.; Oono, Y. *Phys. Lett.* **1982**, *89A*, 460.
(27) Chu, B.; Lee, D.-Ç. *Macromolecules* **1984**, *17*, 926.
(28) Wiltzius, P.; Haller, H. R.; Cannell, S. D. *Phys. Rev. Lett.* **1983**, *51*, 1183.

Application of Raman and Laser Light Scattering to the Solution Polymerization of Hexachlorocyclotriphosphazene. 2.

Benjamin Chu* and Day-chyuan Lee†

Department of Chemistry, State University of New York at Stony Brook, Long Island, New York 11794-3400. *Received November 4, 1985*

ABSTRACT: Poly(dichlorophosphazene) (PDP) can be synthesized by either thermal polymerization of melt hexachlorocyclotriphosphazene (HCTP), as discussed in paper 1, or solution polymerization of HCTP in various solvents. In solution polymerization in the presence of a mixed solvent containing varying amounts of trichlorobenzene (TCB) and HCTP, we have taken into account the effects due to preferential adsorption by refractive index matching of cosolvents that happen to become isorefractive at 110 °C. We have succeeded in determining the molecular parameters, including concentrations of the monomer (C_m) and the polymer (C_p), as well as properties of the polymer product (PDP), such as the weight-average molecular weight (M_w), the second virial coefficients (A_2 and d_d), the z-average radius of gyration (R_g), and the hydrodynamic radius (R_h) in the dilute solution regime, and the cooperative diffusion coefficient (D_c) as well as the osmotic compressibility $[(\partial\pi/\partial C)_{T,P}]$ in semidilute solutions. With precise intensity-intensity time correlation function measurements, we have also succeeded in estimating the polymer molecular weight distribution of PDP during the polymerization process. The development of the present methodology in characterizing PDP in situ avoids the decomposition of PDP by moisture and has the potential to become a practical approach to investigate the solution polymerization of HCTP under a variety of conditions, including judicial use of catalysts. Its eventual development for monitoring specific polymerization processes in situ has become a possibility worthy of consideration.

Introduction

In paper 1, we have shown how thermal polymerization of melt hexachlorocyclotriphosphazene (HCTP) can be monitored in situ by using a combination of laser Raman and light scattering. In our data analysis, we took advantage of Raman spectroscopy to determine the concentration of the polymer (poly(dichlorophosphazene), PDP) in HCTP and a combination of static light scattering intensity and dynamic Rayleigh line width measurements to characterize some of the macromolecular properties of PDP, an important precursor to so many organophosphazene polymers. In this paper (2), we extend our

† Present address: Chemical Engineering Department, University of Wisconsin, Madison, Wisconsin 57305.

0024-9297/86/2219-1592$01.50/0